Journal of Petroleum Research and Studies

Open Access
No. 41, December 2023, pp. 16-36

P- ISSN: 2220-5381
E- ISSN: 2710-1096

DOI: http://doi.org/10.52716/jprs.v13i4.757

Geochemistry and Paleoredox Conditions of The Carbonate Reservoir Khasib Formation in East Baghdad Oilfield-Central Iraq

Rana Abbas Ali
Department of Geology, College of Science, University of Baghdad, Iraq
Corresponding Author E-mail: rana.ali@sc.uobaghdad.edu.iq

Received 19/03/2023, Revised 07/05/2023, Accepted 10/05/2023, Published 12/12/2023

Abstract

The carbonate of Khasib Formation in East Baghdad Oilfield, Central Iraq was geochemically investigated to interpret paleoredox conditions and source of rare earth elements (REEs) based on major, trace, and REEs geochemistry. SiO2 and Al2O3 concentrations are nearly the same in both wells, while CaO content just hardly differs between the EB10 and EB81 cores. The EB10 Well has higher concentrations of Th, Y, and Zr than the EB81 Well. However, both the ∑REE of EB10 (1.969-35.35, n=23) and EB81 (9.59-24.88, n=20) wells have low total REE content. These results show that the Khasib Formation's carbonate sedimentation contains seawater-like marine carbonate and PAAS-normalized REE + Y patterns accompanied by 1- light REE depletion (NdN/YbN= 0.40–0.95, n=23, and 0.54–0.90, n=20, respectively), 2- both positive to negative Ce anomalies (Ce/Ce*= 0.28-1.07, n=23; 0.39-1.76, n=20, respectively), as well as the 3- superchondritic Y/Ho ratio (23.25-57.5, n=23; 18.0-53.0, n=20, respectively). The terrigenous contribution, paleoredox conditions, and scavenging mechanisms were responsible for the observed variations in Ce components and Ce anomalies in the investigated cores. The rising U contents in the limestones (1.62-4.72 ppm) and authigenic U (0.66-4.44 ppm) indicate that dysoxic conditions were present when they were deposited. Further evidence from geochemical data suggests that diagenetic processes may be responsible for the positive Eu anomalies found in limestones. This implies that the Khasib Formation limestones may have kept their original seawater-like REE patterns. Due to trace amounts of detrital materials in certain specimens, there is identified variability in the REE + Y pattern and REE content. The current study shows that the limestones still display their original seawater-like patterns as long as shale contamination was minimal, and they act as a proxy for seawater.

Keywords: Rare earth elements, Limestones, Dysoxic environment, Upper Cretaceous, Ce & Eu anomaly.

Open Access
No. 41, December 2023, pp. 16-36
P- ISSN: 2220-5381
E- ISSN: 2710-1096

1. Introduction:

Carbonate chemical composition reveals physicochemical conditions all through deposition. The major oxides and trace elements supply information on the overall composition of the carbonate reservoirs and depositional environments, allowing us to deduce the nature of the seawater through which they originated. The significance of geochemistry in defining the source area of sedimentary rocks, paleo-weathering conditions, and tectonic evolution of sedimentary basins has been clearly established in numerous research studies [1].

Many researchers have studied the behavior and mode of distribution of rare earth elements (REEs) in carbonate rocks [2]. The research discovered that the most significant factors influencing REE enrichment or depletion through carbonate rocks are: The amounts of terrigenous detrital materials; the variability in seawater oxygen levels; the proximity to the origin area; seawater biogenic deposition; surface productivity variation; diagenesis and lithology; scavenging processes in seawater that are related to oxygen level, salinity, and depth.

The upper Turonian-Lower Coniacian Khasib Formation contains about 14% of the Cretaceous hydrocarbon reserves in Iraq and up to 10% of the entire proven oil reserve [3]. The formation is 60-130 m thick in central Iraq and is prevalent by bioturbated chalky limestones with marlstones, marly limestones and subordinate shales. The formation is widespread in central and southern Iraq, and it serves as a reservoir rock at oilfields such as Samarra, Balad, Tikrit, East Baghdad (Fig. 1). According to Al- Temimi [4], the Khasib Formation has been divided into several units in EB10 (from KB1, 2, 3, 4, 5, and 6), and six units in EB81, that reflects the primary oil-bearing unit in the East Baghdad Oilfield, relying on reservoir characteristics (porosity and saturation). The investigation of sediment cores and log information in Al-Badlawi [5] and Abdel-Fattah et al. [6] studies, based on the detection of micro and electrofacies, revealed that the Khasib Formation deposited in a ramp setting impacted by a transgression event and sea level change.

In this research, we attempted to provide comprehensive information on the source of REEs. In addition, the reasons for the incidence of Eu and Ce anomalies in Khasib Formation limestone using mineralogical and geochemical considerations, as well as determining the depositional environment and forecasting the paleoredox conditions.

2. Geological setting

East Baghdad Oilfield is a regional component of the Arabian Basin, particularly the Mesopotamian Foredeep Basin, which may be evaluating tectonically northeastward towards to

Open Access
No. 41, December 2023, pp. 16-36
P- ISSN: 2220-5381
E- ISSN: 2710-1096

the Zagros Fold Belt, but also westward toward the Widian Basin of Interior Platform, whereas its southern extension is the Mesopotamian Foredeep Basin [7], which contains Neo-Tethys Ocean deposits from the Jurassic & Cretaceous periods. A certain ocean had mostly dysoxic-anoxic palaeoenvironments all along equator and was tectonically unstable. This allowed for the preservation of elevated organic matter and the development of the world's largest oil and gas reserves with in Arabian Province. The lithostratigraphic section consists of marine and sub - ordinates lagoon beds deposited as carbonates, shales, and anhydrites in the southern Neo-Tethys Ocean over a geologic time span spanning the Jurassic, Cretaceous, and Palaeogene periods. In the Mesopotamian Basin, each transgressive-regressive sequence's lateral lithostratigraphic variants and related carbonate bodies (such as prograding shelf margins and forced regressive wedges) could create significant stratigraphic traps [8]. Stratigraphic column of East Baghdad Oilfield is showed in Figure (1 right) [9].

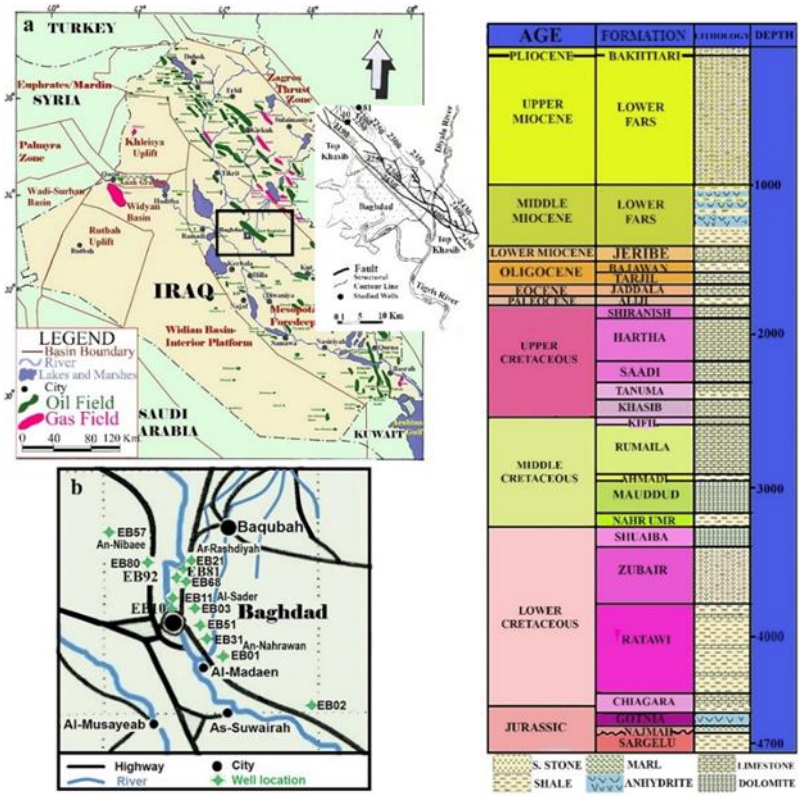

Fig. (1): (a) Position map showing the northeast Arabian Peninsula province of Iraq, along with the locations of basins, oil resources, and boreholes used in this study. (b) The EB10 (East Baghdad 10) and EB81 (East Baghdad 81) wells that were studied are highlighted (left). East Baghdad Oilfield stratigraphic column (right) [9].

Open Access
No. 41, December 2023, pp. 16-36
P- ISSN: 2220-5381
E- ISSN: 2710-1096

3. Materials and methods

This study is based on core and cutting samples from selected oil wells in the East Baghdad Oilfield from the Khasib Formation's Late Turonian - Early Campanian age (Figure 2). The obtained rock samples have been collected at the following locations: 23 samples from EB10 Well at depths of 2134-2235 m, bounded by latitude 37°45′48.4″ North, longitude 43°78′ 53.4″ East, and 20 samples from EB81 Well at depths of 2144-2231 m, bounded by latitude 37°05′13.9″ North, longitude 43°94′97.3″ East, with intervals of 2-8 m. The cores and cuttings employed in this research are identical to those used in [4], which were acquired from the Midland Oil Company in Baghdad.

Following microscopic assessments, reflective limestone cores were selected for chemical analyses. There were some cores to be analyzed containing hydrocarbon materials, so it was necessary to remove them. In the research labs of the Iraqi Ministry of Science and Technology, these samples then were analyzed for major, trace using XRF and REE by atomic absorption spectrometer (SHIMADZU PG-990) methods. In the current study, the correlating values were normalized to typical marine carbonate & PAAS, and calculated Cerium (Ce) and Europium (Eu) anomalies using the following formulas for better interpretation:

$$Ce/Ce^{*} = 2Ce_N/(La_N + Pr_N) \quad (1)$$

$$Eu/Eu^{*} = Eu_N/[(Sm_N \times Gd_N)]^{1/2} \quad (2)$$

$$Pr/Pr^{*} = 2Pr_N/(Ce_N + Nd_N) \quad (3)$$

N denotes the normalization of REEs to marine carbonate [10] and PAAS [1].

Open Access
No. 41, December 2023, pp. 16-36
P- ISSN: 2220-5381
E- ISSN: 2710-1096

4. Results and discussions

4.1 Elemental variations

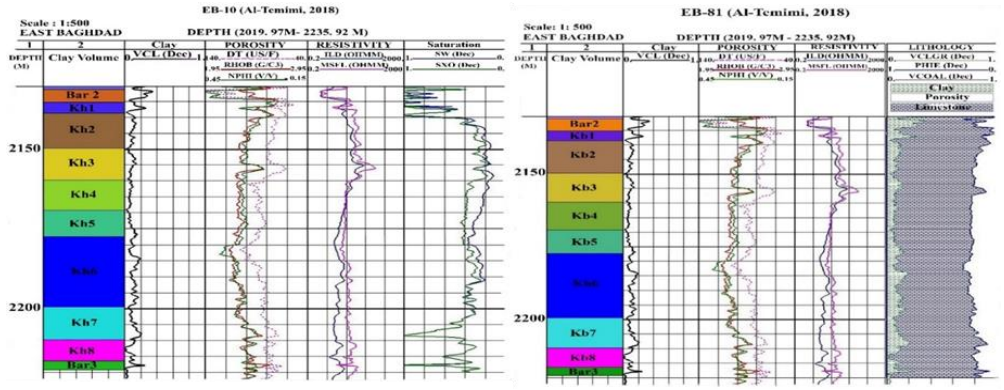

Fig. (2): Log types used to depict the stragraphic boundaries of the Khasib Formation in well EB10 (left); log types that show the lithology of Khasib Formations in well EB81(right).

Table (1) shows the major oxide concentrations in the EB10 and EB81 wells. Both wells have nearly identical SiO_2 and Al_2O_3 contents (5.695% and 1.946% for EB-10; 5.327% and 1.845% for EB81, respectively). TiO_2 levels in the EB10 cores are higher (0.080%) than in the EB81 cores (0.058%). CaO content varies little between the EB10 and EB81 core samples (42.00- 54.32% and 45.36- 51.52%, respectively). The EB10 cores have large variations in MgO and Fe_2O_3 contents (0.50- 2.36% and 0.16- 5.60%, respectively), whereas the EB81 cores have small variations (0.60- 1.93% and 0.17- 1.48 %, respectively). The limestone samples contain very little Na_2O, K_2O, and P_2O_5.

The abundance of CaO among the major elements indicates that $CaCO_3$ has been precipitated straight from seawater in the Khasib carbonate, and the dominance of CaO over MgO indicates that the current carbonate phase is primarily calcite [1]. The reduced MgO content in Khasib carbonate indicates a less saline environment and/or the effect of freshwater diagenesis, which causes extensive leaching in the later phases of diagenesis.

When compared to phases containing other trace elements, common mineral phases that host high field strength elements (HFSE) such as Th, Y, and Zr are resistant to weathering [1]. The EB10 well limestone has higher concentrations of Th, Y, and Zr than the EB81 well limestone (Table 2). Khasib carbonate limestone have low Co, Pb, and Sc contents.

Journal of Petroleum Research and Studies

Open Access
No. 41, December 2023, pp. 16-36

P- ISSN: 2220-5381
E- ISSN: 2710-1096

Table (1) A list of concentration of major oxides (wt.%) of cores taken from the Khasib Fm. limestone of EB10 and EB81 wells

Well No.	Core No.	Depth m.	SiO_2	Al_2O_3	Fe_2O_3	CaO	MgO	Na_2O	K_2O	TiO_2	P_2O_5	LOI	Total
EB10	Kh_1	2134	4.33	1.17	0.63	51.52	1.90	0.11	0.09	0.03	0.03	39.3	99.11
	Kh_2	2140	7.15	5.36	5.60	42.00	2.36	0.08	0.82	0.17	0.09	35.9	99.51
	Kh_3	2142	3.52	1.08	0.42	51.52	1.33	0.05	0.23	0.03	0.03	41.2	99.41
	Kh_4	2146	5.44	1.34	0.31	50.4	0.63	0.13	0.25	0.04	0.03	40.7	99.27
	Kh_5	2150	4.18	1.55	0.16	51.24	0.50	0.11	0.08	0.03	0.04	41.6	99.49
	Kh_6	2154	7.12	3.66	0.28	42.00	0.56	0.14	0.68	0.19	0.08	45.2	99.93
	Kh_7	2158	3.32	0.35	0.17	54.32	0.53	0.09	0.03	0.02	0.03	40.3	99.16
	Kh_8	2164	4.95	1.66	0.20	49.64	0.53	0.06	0.37	0.05	0.03	41.8	99.31
	Kh_9	2170	4.00	1.54	0.19	51.24	0.60	0.09	0.19	0.06	0.04	41.6	99.55
	Kh_{10}	2176	5.86	1.57	0.19	50.40	0.66	0.15	0.22	0.12	0.04	40.4	99.61
	Kh_{11}	2180	4.67	1.56	0.26	50.12	0.66	0.19	0.18	0.03	0.04	41.7	99.41
	Kh_{12}	2186	4.39	1.75	0.34	49.28	0.73	0.20	0.21	0.07	0.06	42.8	99.83
	Kh_{13}	2194	5.42	1.05	0.2	50.40	0.66	0.15	0.09	0.07	0.05	41.3	99.39
	Kh_{14}	2200	7.66	1.36	0.57	48.16	0.76	0.05	0.07	0.09	0.06	40.3	99.08
	Kh_{15}	2206	4.78	0.75	0.54	52.08	0.90	0.17	0.06	0.03	0.03	40.6	99.94
	Kh_{16}	2210	4.55	1.55	0.34	50.40	0.70	0.19	0.13	0.03	0.03	41.7	99.62
	Kh_{17}	2212	4.74	1.45	2.00	49.28	0.73	0.11	0.09	0.07	0.04	40.6	99.11
	Kh_{18}	2216	5.54	2.80	0.30	46.20	0.83	0.20	0.61	0.09	0.07	42.6	99.24
	Kh_{19}	2220	5.22	1.77	0.37	50.40	0.76	0.23	0.73	0.04	0.03	40.3	99.85
	Kh_{20}	2224	4.77	2.11	0.24	48.72	0.73	0.16	0.83	0.19	0.07	41.4	99.22
	Kh_{21}	2228	5.32	2.32	0.28	49.00	0.86	0.06	0.14	0.08	0.03	41.5	99.59
	Kh_{22}	2230	7.85	1.75	0.34	47.60	0.80	0.12	0.76	0.05	0.07	40.3	99.64
	Kh_{23}	2235	10.72	3.66	1.94	42.28	0.96	0.01	0.83	0.19	0.09	38.5	99.20
EB81	Kb_1	2144	5.72	1.66	0.22	50.55	0.66	0.06	0.15	0.04	0.04	40.2	99.71
	Kb_2	2148	6.21	1.98	0.23	49.84	0.73	0.03	0.24	0.06	0.03	40.4	99.75
	Kb_3	2150	3.32	1.07	0.31	50.96	0.66	0.04	0.22	0.05	0.03	42.5	99.16
	Kb_4	2154	5.45	1.35	0.51	50.40	0.73	0.07	0.21	0.07	0.04	40.6	99.43
	Kb_5	2160	4.79	1.34	0.71	50.72	0.66	0.05	0.14	0.05	0.03	40.5	99.23
	Kb_6	2163	3.78	1.05	0.23	51.52	0.60	0.09	0.09	0.04	0.04	41.7	99.14
	Kb_7	2167	4.82	2.08	0.18	50.89	0.73	0.10	0.16	0.03	0.03	40.4	99.49
	Kb_8	2174	3.84	1.35	0.57	51.52	0.73	0.15	0.11	0.04	0.03	41.5	99.84
	Kb_9	2180	4.73	1.12	0.28	50.40	0.92	0.02	0.13	0.05	0.04	41.8	99.49
	Kb_{10}	2183	5.64	1.32	0.34	49.84	0.86	0.20	0.19	0.07	0.06	41.2	99.72
	Kb_{11}	2188	6.55	2.32	1.23	48.72	0.81	0.11	0.05	0.04	0.07	40.0	99.90
	Kb_{12}	2191	4.65	1.76	1.48	49.84	0.90	0.23	0.27	0.05	0.05	40.2	99.43
	Kb_{13}	2195	5.34	1.54	0.85	49.28	0.66	0.12	0.17	0.06	0.05	41.4	99.47
	Kb_{14}	2203	4.75	1.95	0.42	49.75	0.74	0.15	0.06	0.07	0.06	42.3	99.78
	Kb_{15}	2209	6.55	2.69	0.28	48.72	0.76	0.10	0.19	0.04	0.07	40.2	99.60
	Kb_{16}	2212	4.73	1.96	0.20	50.40	1.93	0.03	0.12	0.03	0.03	40.2	99.63
	Kb_{17}	2217	5.88	1.76	0.17	48.16	1.20	0.08	0.17	0.04	0.07	41.5	99.03
	Kb_{18}	2223	7.42	3.66	0.20	45.36	0.66	0.09	0.07	0.12	0.09	41.6	99.27
	Kb_{19}	2229	5.62	1.11	0.19	50.40	0.81	0.04	0.18	0.09	0.03	41.2	99.67
	Kb_{20}	2231	4.65	1.77	0.29	49.84	0.85	0.05	0.09	0.05	0.04	41.7	99.33

Open Access
No. 41, December 2023, pp. 16-36
P- ISSN: 2220-5381
E- ISSN: 2710-1096

Table (2) A list of concentration of trace elements (ppm) of cores taken from the Khasib Fm. limestone of EB10 and EB81 wells

Well No.	Core No.	Depth m.	V	Cr	Co	Ni	Rb	Ba	Sr	Th	U	Cu	Y	Zr	Pb	Zn	Mn	Sc
EB10	Kh_1	2134	26	33	1.55	60	8.85	7.9	360	0.74	2.81	150	5.35	7.12	1.50	45	129	0.47
	Kh_2	2140	34	7	2.80	40	6.64	20.0	320	2.41	3.21	10	7.5	35.0	0.83	10	119	2.90
	Kh_3	2142	32	23	1.26	160	3.86	7.0	200	0.27	2.71	145	4.45	9.56	2.50	30	65	1.04
	Kh_4	2146	30	36	2.22	45	5.39	4.4	160	0.53	2.59	125	3.53	8.52	3.52	40	315	1.10
	Kh_5	2150	28	33	1.57	44	6.55	75.0	240	1.42	2.75	130	4.78	0.50	0.95	70	127	0.72
	Kh_6	2154	14	34	2.55	46	7.97	10.0	350	2.09	4.5	10	8.0	2.20	0.78	130	117	2.20
	Kh_7	2158	36	44	1.19	42	0.72	1.5	260	0.09	1.62	199	1.15	2.73	1.59	90	165	0.12
	Kh_8	2164	30	22	2.47	46	9.52	17.4	220	1.22	2.84	165	4.59	5.57	0.95	55	170	1.00
	Kh_9	2170	30	23	2.98	50	4.42	9.8	280	2.79	2.19	135	4.75	7.15	0.96	80	137	1.02
	Kh_{10}	2176	26	35	4.32	40	12.34	20.0	440	1.26	2.65	126	4.53	0.63	1.75	88	257	1.12
	Kh_{11}	2180	34	25	1.45	40	10.35	18.2	280	0.55	2.21	105	2.65	7.62	1.58	70	170	1.11
	Kh_{12}	2186	20	29	2.75	48	9.92	30.0	370	1.52	3.85	189	4.98	8.34	1.96	66	125	1.05
	Kh_{13}	2194	18	33	1.66	45	9.53	40.0	380	0.33	4.55	155	4.5	7.34	4.52	90	150	0.92
	Kh_{14}	2200	30	27	3.82	40	3.14	45.0	325	1.44	4.72	149	5.57	2.55	0.75	75	93	0.95
	Kh_{15}	2206	20	19	1.43	40	2.33	80.0	340	0.38	1.73	200	2.48	0.44	2.12	98	178	0.47
	Kh_{16}	2210	22	24	2.46	60	10.4	55.0	280	0.65	1.45	175	4.75	4.80	3.15	95	110	1.10
	Kh_{17}	2212	32	26	4.62	65	9.52	50.0	290	0.72	2.27	25	4.79	7.50	0.92	78	154	1.11
	Kh_{18}	2216	50	40	4.23	40	3.54	17.0	320	1.75	4.32	45	5.85	1.40	1.44	140	106	2.20
	Kh_{19}	2220	16	38	3.35	50	10.52	12.0	300	0.55	1.75	190	2.79	0.50	2.50	73	75	1.12
	Kh_{20}	2224	24	35	2.75	45	4.54	44.0	280	1.23	2.25	157	5.17	7.20	1.95	109	121	1.15
	Kh_{21}	2228	14	30	1.49	30	8.25	38.0	240	0.74	2.35	164	3.75	0.90	1.77	97	98	1.00
	Kh_{22}	2230	15	34	2.45	35	5.28	79.0	230	2.44	3.74	177	5.74	1.70	1.75	103	137	2.00
	Kh_{23}	2235	18	44	3.94	35	12.52	60.0	200	5.45	4.40	20	9.6	37.0	4.50	25	97	2.50
EB81	Kb_1	2144	32	25	1.45	40	4.65	33.0	300	0.32	2.77	120	2.89	7.62	0.95	65	155	0.94
	Kb_2	2148	40	20	1.35	35	5.49	15.3	240	1.12	3.79	150	3.38	9.45	3.52	55	193	1.07
	Kb_3	2150	40	10	1.79	80	4.98	9.8	320	0.45	2.25	158	4.25	0.70	1.41	10	259	0.74
	Kb_4	2154	32	44	2.57	65	8.83	5.1	480	0.57	0.85	195	3.47	5.20	0.94	79	170	1.10
	Kb_5	2160	24	16	2.92	60	4.79	7.0	400	0.72	4.3	180	4.77	7.13	0.78	37	129	0.72
	Kb_6	2163	28	20	2.82	70	9.75	78.0	640	1.72	2.65	205	3.90	10.5	2.50	85	187	1.05
	Kb_7	2167	28	18	2.52	75	5.44	8.5	330	2.24	2.95	119	4.05	4.50	1.44	81	90	0.57
	Kb_8	2174	33	27	3.67	14	6.52	45.0	250	1.63	2.55	197	4.38	0.70	0.79	88	97	1.02
	Kb_9	2180	17	22	3.82	25	9.34	16.2	350	0.64	1.79	178	2.52	5.00	0.92	35	189	1.00
	Kb_{10}	2183	32	20	1.35	38	9.35	30.0	400	0.55	1.09	165	4.22	2.42	1.77	25	173	0.63
	Kb_{11}	2188	20	40	2.84	40	3.12	20.0	340	1.52	2.75	75	4.12	2.50	2.30	49	107	0.90
	Kb_{12}	2191	20	25	1.78	80	7.52	55.0	320	1.44	2.95	174	4.72	5.46	1.66	69	253	0.95
	Kb_{13}	2195	16	36	3.54	44	10.25	70.0	310	1.95	2.82	188	3.52	8.20	1.85	78	221	1.20
	Kb_{14}	2203	27	18	2.58	80	8.42	66.0	340	1.90	2.95	165	3.54	3.00	1.33	77	65	1.40
	Kb_{15}	2209	19	35	2.32	75	4.52	12.0	240	2.42	3.92	130	4.89	1.40	2.70	64	93	1.07
	Kb_{16}	2212	16	27	1.36	30	5.72	18.5	550	0.49	0.91	199	3.12	4.52	0.90	33	127	0.82
	Kb_{17}	2217	24	35	3.23	35	10.53	22.0	320	2.20	2.82	184	4.75	0.40	1.50	58	73	0.95
	Kb_{18}	2223	28	33	3.42	34	7.72	25.0	330	3.15	4.42	120	7.92	34.0	4.50	95	137	2.00
	Kb_{19}	2229	20	20	1.89	50	5.72	5.7	550	0.57	2.98	190	3.55	5.65	1.00	91	133	1.02
	Kb_{20}	2231	20	20	2.49	65	8.44	35.0	310	0.66	2.55	183	2.35	7.53	1.70	72	170	1.09

The EB10 well has large variations in Ba, V, and Rb contents, whereas the EB81 well has the smallest variations. The Cu, Zn, and U contents of the EB10 and EB81 wells vary the least. The Sr contents of the EB10 and EB81 core samples (160-440 ppm and 240-640 ppm, respectively) are slightly lower than the typical value for lithosphere carbonates (Sr= 610 ppm, [10]).

Bivariate plots of major element pairs (see data in table 1) show that correlation coefficients are positive and weak for SiO2-Al2O3 (R2= 0.416) (Fig. 3a), SiO2- Fe2O3 (R2= 0.108) has a positive and weak correlation (Fig. 3b), CaO-Al2O3 (R2= - 0.808) has a negative and strong correlation (Fig. 3c), CaO-Fe2O3 has a negative and weak correlation (R2= -0.277) (Fig. 3d), TiO2-Al2O3

Open Access
No. 41, December 2023, pp. 16-36
P- ISSN: 2220-5381
E- ISSN: 2710-1096

(R2= 0.47) has a positive and weak correlation (Fig. 3e), TiO2-Fe2O3 (R2= 0.080) has a positive and weak correlation (Fig. 3f), SiO2-CaO has a negative and strong correlation (R2= -0.626) (Fig. 3g), positive and weak forTiO2-SiO2 (R2= 0.182) (Fig. 3h). These chart shows that CaO has a completely different origin from the other component oxides of the limestone.

The cores of the Khasib limestone exhibit weak depletion in comparing to marine carbonate [10], as well as significant enrichment for elements like V, Ni, Rb, and Sc; for elements like Co, Ba, Sr, Y, Zr, Pb, and Mn, there is a severe depletion; there has been a notable enrichment for the elements Cr, Cu, and Zn for EB10 (Fig. 4).

The analyzed limestone's ∑REE values range from 1.969 to 35.350 ppm for EB10 and 9.590 to 24.880 ppm for EB81, respectively. These values demonstrate both depletion and enrichment patterns in comparing to the typical marine carbonate [10] (Fig.5). For EB10, the values of Eu/Eu* and Ce/Ce* have respective ranges of 0.45–1.82 and 0.28–1.07; 0.66–1.73 and 0.39–1.76 for EB81 (Table 4).

4.2 The limestone's source of REEs

Since limestone typically have lower REE concentrations than shales, it is likely that marine carbonate phases have significantly lower REE concentrations than terrigenous materials [11]. While terrigenous sediments have relatively high REE concentrations and patterns that are unlike those found in seawater, which contributes a lower concentration of REE. The following aspects are visible in seawater-like REE + Y patterns normalized by PAAS: considerable LREE depletion, negatively Ce anomaly, faint positive La anomalous, as well as superchondritic Y/Ho ratios [12]. Both EB10 and EB81 contain little total REE (Table 3). Most limestone exhibit 1- LREE depletion and PAAS- normalized seawater-like REE+ Y trends (Fig.6; NdN/YbN= 0.40- 0.95, and 0.54- 0.90 for EB10 and EB81, respectively); 2- Ce/Ce*= 0.28–1.07 and 0.39–1.76 for EB10 and EB81, respectively, measure both positive and negative Ce anomalies; 3- positive anomalies with La (La/La*= 0.48–4.33 and 0.30–1.92 for EB10 and EB81, respectively); 4- increased Y/Ho ratio (23.43- 57.50 and 18.00- 53.00 for EB10 and EB81, respectively) (Table 4).

Recent studies demonstrated that by taking into account the correlation coefficients between specific trace and major elements and REEs, it is possible to identify the contributing of terrigenous source for REEs in limestone. Si, Al, Ti, K, P, Cr, Sc, V, Rb, Th, Zr, Ni, Y, and Co are frequently positively correlated with detrital-derived REEs, while Ca is typically negatively correlated with

Open Access
No. 41, December 2023, pp. 16-36
P- ISSN: 2220-5381
E- ISSN: 2710-1096

these elements [13]. Analysis of the correlation coefficients between the elements in the Khasib limestone reveals that the REEs have positive correlations with SiO2 (R2= 0.556; Fig.7a), Al2O3 (R2= 0.762; Fig.7b), TiO2 (R2= 0.561; Fig.7d), P2O5 (R2= 0.668; Fig.7e), Cr (R2= 0.02; Fig.7f), Rb (R2= 0.036; Fig.7g), Th (R2= 0.559; Fig.7h), Zr (R2= 0.407; Fig.7i), and Co (R2= 0.15; Fig.7j), while a negative correlation (R2= -0.876; Fig. 7c) with CaO. These connections imply a few detrital influence on the REE contents of the sample. Because of the greater REE concentration in detrital particles and the generally flat REE pattern typical of common detrital materials. Seawater signatures can be effectively preserved in carbonate rocks while maintaining their original seawater-like REE patterns.

One limestone specimen (Kh7) of the EB10 well has a relatively low ∑REE content (1.969 ppm) as well as LREE depletion inside the typical range for modern seawater (NdN/YbN = 0.4; contemporary shallow water = 0.205– 0.492 for 50 m water depth). If PAAS and the reduced ∑REE limestone sample are mixed cautiously, the extent that the detrital content impacts the REE patterns in the EB10 and EB81 could be assessed (Kh7). Due to its low ∑REE content, important LREE depletion, REE pattern resembling that of modern seawater, and superchondritic Y/Ho ratio, the limestone specimen (Kh7) can be regarded as the least clastic input-contaminated and used as a seawater-like content. Shale has a rising REE concentration, and adding even 1% to 2% of fine-grained material could dramatically change the LREE depletion, Ce anomalies, and REE patterns [14].

Additionally, the limestones with higher REE concentrations (5.05–35.35 ppm) display distinctive REE + Y patterns that resemble seawater. Just a small amount of REE from terrigenous materials (less 5 % of local shale contamination) contributes to the seawater-like REE + Y patterns found within those limestones, which are primarily caused by the absorption of REE from current seawaters. Therefore, the ancient limestones deposited inside the proximal portion of the basin with very little detrital material are appropriate to comprehend the REE patterns of ancient shallow seawater as well as act as an important seawater proxy.

4.4 Ce anomaly

It has been thought that the Ce anomalies in marine carbonate rocks are an appropriate indicator for comprehending the current paleoredox conditions [14]. Comparable Ce anomalies in limestone discover the incorporation of REEs +Y straight from seawater or pore water under oxic conditions, just as marine water exhibits a negative Ce anomaly. The scarcity of Ce in comparison to nearby

Open Access
No. 41, December 2023, pp. 16-36
P- ISSN: 2220-5381
E- ISSN: 2710-1096

rare earth elements is a significant characteristic of contemporary seawater. This could be clarified by the oxidation of trivalent cerium to the less soluble tetravalent cerium and also the subsequent removal of the cerium by suspended molecules through the scavenging system [15]. A less negative to positive anomaly in seawater results from Ce being remobilized and released into the water column in a suboxic to anoxic environment. However, accurate measurements of the redox conditions at the time and location of deposition may be limited by Ce anomalies throughout marine sediments.

Using Bau and Dulski's [16] plot of Ce/Ce*"equation (1)," vs. Pr/Pr*"equation (3)", Ce and La anomalies have been computed. The majority of the data display negative Ce and positive La anomalies, while only a small number of specimens don't show negative Ce anomalies (Figure 8). Ce/Ce* ratio depends on the ratios of clastic contamination and pure seawater precipitate in these two cores, in addition to their respective REEs + Y concentrations. The Ce/Ce* ratio gets closer to 1 as clastic contamination rises (Table 4). Ce/Ce* values in seawater vary between 0.1 and 0.4 [14]. Fewer limestone samples exhibit positive Ce anomalies, which are primarily caused by paleoredox conditions, terrigenous input, diagenesis [14], scavenging process [17], while more limestone samples exhibit negative Ce anomalies.

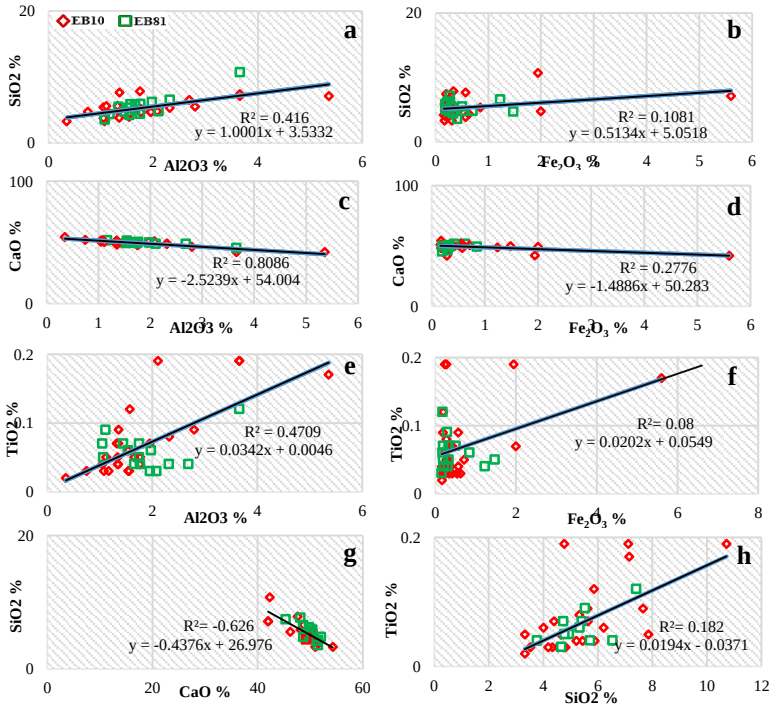

Fig. (3): Bivariate plot points for sets of (a) SiO_2-Al_2O_3, (b) SiO_2-Fe_2O_3, (c) CaO- Al_2O_3, (d) CaO- Fe_2O_3, (e) TiO_2- Al_2O_3, f) TiO_2- Fe_2O_3, (g) SiO_2- CaO, and (h) TiO_2-SiO_2 in Khasib Fm. limestone.

Open Access
No. 41, December 2023, pp. 16-36

P- ISSN: 2220-5381
E- ISSN: 2710-1096

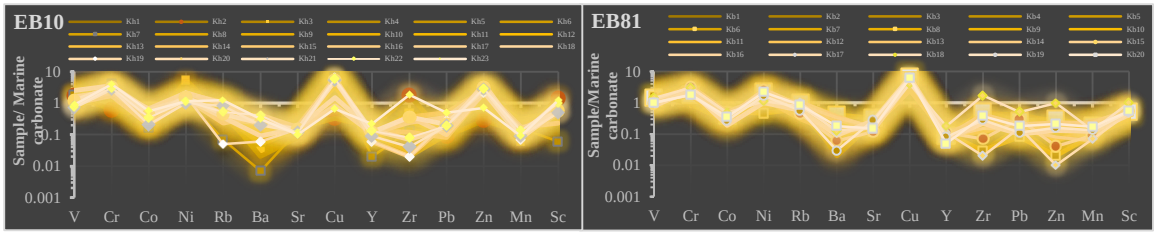

Fig. (4): The distribution patterns for trace elements of cores taken from the limestone of Khasib Fm, normalized to marine carbonate [10].

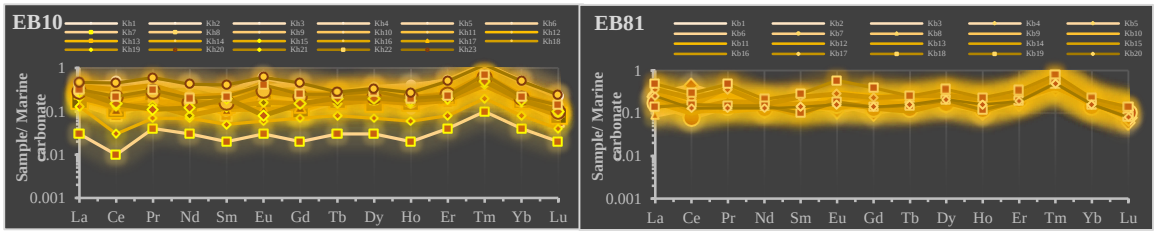

Fig. (5): The distribution patterns for REEs of cores taken from the limestone of Khasib Fm, normalized to marine carbonate [10].

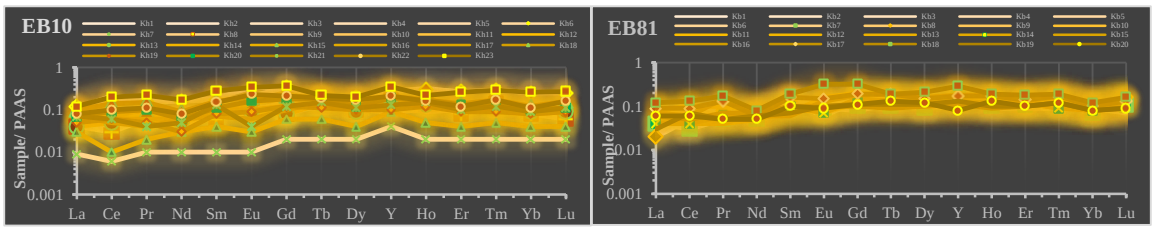

Fig. (6): The distribution patterns for REEs of cores taken from the limestone of Khasib Fm, normalized to PAAS [1].

Open Access
No. 41, December 2023, pp. 16-36

P- ISSN: 2220-5381
E- ISSN: 2710-1096

Table (3) A list of concentration of rare earth elements (ppm) of cores taken from the Khasib Fm. limestone of EB10 and EB81 wells

Well No.	Core No.	Depth m.	LREE						HREE								∑REE
			La	Ce	Pr	Nd	Sm	Eu	Gd	Tb	Dy	Ho	Er	Tm	Yb	Lu	
EB10	Kh_1	2134	2.57	4.52	0.54	2.75	0.50	0.12	0.50	0.11	0.51	0.14	0.27	0.05	0.36	0.05	12.99
	Kh_2	2140	4.29	17.02	1.54	5.71	1.09	0.37	1.51	0.17	0.97	0.32	0.75	0.12	0.75	0.11	34.72
	Kh_3	2142	2.22	3.55	0.72	2.38	0.60	0.10	0.55	0.13	0.52	0.14	0.34	0.05	0.31	0.05	11.66
	Kh_4	2146	2.14	5.72	0.55	1.75	0.52	0.10	0.41	0.10	0.50	0.12	0.35	0.04	0.25	0.04	12.59
	Kh_5	2150	1.72	3.49	0.52	2.05	0.54	0.11	0.54	0.09	0.54	0.12	0.30	0.04	0.25	0.04	10.35
	Kh_6	2154	4.71	12.7	1.33	5.71	0.97	0.23	1.62	0.15	0.95	0.30	0.79	0.12	0.72	0.11	30.41
	Kh_7	2158	0.35	0.54	0.14	0.44	0.09	0.019	0.09	0.02	0.10	0.02	0.07	0.01	0.07	0.01	1.969
	Kh_8	2164	1.55	3.00	0.57	2.17	0.37	0.112	0.40	0.12	0.47	0.14	0.25	0.06	0.24	0.03	9.482
	Kh_9	2170	2.37	3.74	0.71	2.19	0.53	0.11	0.57	0.10	0.53	0.13	0.31	0.04	0.25	0.04	11.62
	Kh_{10}	2176	1.42	4.50	0.60	2.38	0.40	0.113	0.74	0.09	0.49	0.09	0.29	0.05	0.27	0.04	11.473
	Kh_{11}	2180	2.65	5.25	0.71	1.55	0.48	0.07	0.53	0.10	0.48	0.10	0.32	0.06	0.24	0.04	12.58
	Kh_{12}	2186	2.05	5.47	0.62	2.13	0.57	0.10	0.45	0.13	0.57	0.14	0.35	0.04	0.25	0.05	12.92
	Kh_{13}	2194	1.82	4.01	0.55	1.95	0.55	0.10	0.39	0.11	0.42	0.13	0.33	0.05	0.27	0.04	10.72
	Kh_{14}	2200	2.54	5.75	0.96	2.79	0.45	0.17	0.90	0.14	0.59	0.17	0.38	0.06	0.30	0.05	15.25
	Kh_{15}	2206	1.37	1.25	0.25	1.04	0.22	0.04	0.30	0.05	0.20	0.05	0.12	0.02	0.12	0.02	5.05
	Kh_{16}	2210	2.84	4.70	0.57	2.17	0.57	0.11	0.56	0.10	0.51	0.12	0.30	0.05	0.25	0.04	12.89
	Kh_{17}	2212	2.67	4.10	0.40	2.12	0.42	0.07	0.47	0.12	0.58	0.15	0.32	0.05	0.27	0.05	11.79
	Kh_{18}	2216	3.82	11.2	1.32	3.17	0.92	0.22	1.02	0.15	0.75	0.17	0.40	0.07	0.35	0.07	23.63
	Kh_{19}	2220	2.12	4.77	0.48	1.20	0.47	0.10	0.57	0.09	0.50	0.12	0.27	0.04	0.24	0.04	11.01
	Kh_{20}	2224	2.79	7.51	0.95	2.26	0.62	0.18	0.85	0.14	0.57	0.17	0.37	0.06	0.30	0.05	16.82
	Kh_{21}	2228	2.95	5.32	0.38	1.75	0.77	0.05	0.58	0.12	0.55	0.15	0.30	0.05	0.27	0.05	13.29
	Kh_{22}	2230	3.22	7.93	1.05	2.92	0.87	0.25	0.95	0.15	0.79	0.16	0.35	0.07	0.33	0.07	19.11
	Kh_{23}	2235	4.77	15.92	1.98	5.94	1.58	0.37	1.72	0.17	0.94	0.22	0.75	0.12	0.75	0.12	35.35
EB81	Kb_1	2144	2.56	5.49	0.71	2.19	0.55	0.11	0.55	0.09	0.53	0.12	0.32	0.06	0.25	0.05	13.58
	Kb_2	2148	1.72	4.05	0.57	2.44	0.57	0.09	0.72	0.10	0.58	0.13	0.35	0.06	0.29	0.05	11.72
	Kb_3	2150	2.07	3.75	0.65	2.20	0.72	0.10	0.65	0.11	0.59	0.12	0.38	0.05	0.25	0.05	11.69
	Kb_4	2154	2.75	4.40	0.78	1.97	0.67	0.07	0.62	0.12	0.54	0.09	0.33	0.04	0.27	0.03	12.68
	Kb_5	2160	2.47	3.09	0.59	1.75	0.75	0.10	0.39	0.09	0.45	0.09	0.27	0.04	0.24	0.04	10.36
	Kb_6	2163	0.89	4.57	0.74	2.85	0.59	0.12	0.70	0.11	0.72	0.15	0.39	0.06	0.32	0.06	12.27
	Kb_7	2167	1.78	2.96	0.47	1.85	0.65	0.10	0.50	0.08	0.46	0.10	0.32	0.05	0.22	0.05	9.59
	Kb_8	2174	0.95	7.35	0.75	2.57	0.74	0.134	0.74	0.10	0.62	0.15	0.37	0.06	0.33	0.07	14.934
	Kb_9	2180	2.35	6.55	0.58	1.95	0.62	0.12	0.65	0.09	0.49	0.14	0.28	0.04	0.25	0.04	14.147
	Kb_{10}	2183	2.82	5.57	0.52	2.00	0.52	0.08	0.59	0.13	0.55	0.16	0.35	0.05	0.25	0.07	13.66
	Kb_{11}	2188	3.24	7.93	0.88	2.77	0.42	0.18	0.97	0.14	0.75	0.17	0.41	0.07	0.32	0.07	18.32
	Kb_{12}	2191	3.05	4.20	0.39	1.94	0.49	0.09	0.54	0.10	0.59	0.12	0.29	0.06	0.22	0.06	12.14
	Kb_{13}	2195	1.97	3.88	0.40	2.45	0.53	0.09	0.58	0.11	0.65	0.10	0.34	0.04	0.27	0.07	11.482
	Kb_{14}	2203	1.81	3.79	0.52	2.20	0.58	0.09	0.73	0.10	0.67	0.12	0.35	0.04	0.25	0.05	11.295
	Kb_{15}	2209	2.98	5.40	1.33	2.17	0.37	0.14	0.84	0.15	0.76	0.18	0.37	0.07	0.30	0.05	15.11
	Kb_{16}	2212	2.44	4.50	0.65	2.40	0.61	0.112	0.50	0.07	0.50	0.09	0.30	0.05	0.27	0.04	12.532
	Kb_{17}	2217	3.64	7.70	1.21	2.27	0.92	0.17	0.90	0.15	0.72	0.17	0.40	0.07	0.29	0.06	18.67
	Kb_{18}	2223	4.79	10.3	1.55	2.97	1.09	0.35	1.50	0.15	0.98	0.19	0.52	0.08	0.34	0.07	24.88
	Kb_{19}	2229	1.47	5.68	0.51	2.10	0.40	0.115	0.54	0.09	0.54	0.10	0.29	0.05	0.25	0.04	12.175
	Kb_{20}	2231	2.57	4.70	0.44	1.84	0.55	0.097	0.55	0.10	0.57	0.13	0.29	0.05	0.25	0.04	12.177

Table (4) lists the anomalies and elemental ratios found in Khasib Fm. limestone.

Well No.	Core No.	Depth m.	Y/Ho	Er/Nd	La_N/Yb_N	Nd_N/Yb_N	Eu/Eu*	Ce/Ce*	La/La*	Pr/Pr*	Authigenic U (ppm)
EB10	Kh_1	2134	38.21	0.09	1.04	0.90	1.53	0.63	2.50	1.00	2.57
	Kh_2	2140	23.43	0.13	0.86	0.80	1.82	1.07	0.74	1.04	2.41
	Kh_3	2142	31.78	0.14	1.10	0.65	1.10	0.46	0.75	1.55	2.62
	Kh_4	2146	29.41	0.20	1.30	0.75	1.39	0.86	0.87	1.14	2.42
	Kh_5	2150	39.83	0.14	1.06	0.77	1.28	0.62	1.00	1.33	2.28
	Kh_6	2154	26.66	0.13	0.97	0.66	1.13	0.82	1.17	1.05	3.81
	Kh_7	2158	57.50	0.16	0.75	0.40	1.50	0.28	0.50	2.00	1.59
	Kh_8	2164	32.78	0.11	0.93	0.80	1.80	0.50	0.71	1.47	2.44
	Kh_9	2170	36.53	0.14	1.43	0.65	1.24	0.45	0.69	1.68	1.26
	Kh_{10}	2176	50.33	0.12	0.77	0.85	1.24	0.75	0.70	1.24	2.23
	Kh_{11}	2180	26.50	0.20	1.62	0.74	0.84	0.63	0.63	1.61	2.03
	Kh_{12}	2186	35.57	0.16	1.25	0.64	1.23	0.79	0.83	1.20	3.35
	Kh_{13}	2194	34.61	0.17	1.00	0.85	1.33	0.64	0.90	1.28	4.44
	Kh_{14}	2200	32.76	0.13	1.25	0.88	1.64	0.59	0.51	1.65	4.24
	Kh_{15}	2206	49.60	0.11	1.62	0.75	1.00	0.30	1.85	1.40	1.61
	Kh_{16}	2210	39.58	0.13	1.75	0.80	1.24	0.57	1.33	1.21	1.24

Open Access
No. 41, December 2023, pp. 16-36
P- ISSN: 2220-5381
E- ISSN: 2710-1096

EB81	Kh_{17}	2212	31.93	0.15	1.44	0.67	0.95	0.57	4.33	0.92	2.03
	Kh_{18}	2216	34.41	0.12	1.65	0.72	1.44	0.82	0.50	1.48	3.74
	Kh_{19}	2220	23.25	0.22	1.31	0.75	1.18	0.74	0.80	1.33	1.57
	Kh_{20}	2224	30.41	0.16	1.40	0.95	1.18	0.75	0.53	1.51	1.84
	Kh_{21}	2228	25.00	0.17	1.61	0.90	0.45	0.75	3.22	0.81	2.11
	Kh_{22}	2230	35.87	0.12	1.45	0.84	0.45	0.69	0.60	1.47	2.93
	Kh_{23}	2235	43.63	0.12	0.94	0.70	1.41	0.84	0.48	1.37	2.59
	Kb_{1}	2144	24.08	0.14	1.56	0.68	1.28	0.65	0.75	1.40	2.67
	Kb_{2}	2148	26.0	0.14	0.89	0.76	0.88	0.64	1.00	1.21	3.42
	Kb_{3}	2150	35.41	0.17	1.25	0.70	0.88	0.51	0.74	1.52	2.10
	Kb_{4}	2154	38.55	0.16	1.50	0.85	0.66	1.76	0.65	0.79	0.66
	Kb_{5}	2160	53.0	0.15	1.50	0.89	1.10	0.39	0.88	1.70	4.06
	Kb_{6}	2163	26.0	0.13	0.42	0.75	1.21	0.83	0.34	1.33	2.08
	Kb_{7}	2167	40.5	0.17	1.70	0.66	1.06	0.51	1.06	1.33	2.21
	Kb_{8}	2174	29.2	0.14	0.40	0.92	1.10	1.35	0.30	1.12	2.04
	Kb_{9}	2180	18.0	0.14	1.43	0.55	1.09	0.90	1.00	1.06	1.58
	Kb_{10}	2183	26.37	0.17	1.75	0.54	0.92	0.74	1.64	1.00	0.91
	Kb_{11}	2188	24.23	0.14	1.52	0.75	1.66	0.75	0.80	1.26	2.25
	Kb_{12}	2191	39.33	0.15	2.14	0.80	1.15	0.58	2.28	0.88	2.47
	Kb_{13}	2195	35.2	0.13	1.05	0.77	1.03	0.71	1.77	0.85	2.17
	Kb_{14}	2203	29.5	0.16	1.12	0.72	0.76	0.57	0.85	1.36	2.32
	Kb_{15}	2209	27.16	0.17	1.45	0.85	1.48	0.43	0.32	2.66	3.12
	Kb_{16}	2212	34.66	0.12	1.33	0.84	1.24	0.79	1.04	1.31	0.75
	Kb_{17}	2217	27.94	0.17	1.89	0.85	1.19	0.61	0.47	1.89	2.09
	Kb_{18}	2223	41.68	0.17	2.18	0.9	1.73	0.61	0.48	1.88	3.37
	Kb_{19}	2229	35.5	0.13	0.87	0.57	1.50	1.10	0.93	0.96	2.79
	Kb_{20}	2231	18.67	0.15	1.56	0.69	1.14	0.68	1.92	1.00	2.33

The Ce/Ce* values in the current study have a weak positive correlation with scavenging-type particle reactive elements, such as Fe and Mn (R^2 = 0.0400 and 0.0007, respectively) (Figure 9 a, b). These correlations demonstrate that the limestone under study precipitated inside a shallow marine deposition environment, in which the role of scavenging processes is relatively less significant than in deep marine environments. In some situations, the redox potential of Fe or/and Mn may also be related to Ce distribution. Using other redox sensitive elements (such as uranium content and uranium produced authigenically), it is possible to test whether the variations in Ce anomalies are caused by scavenging processes or paleo-redox changes.

Open Access
No. 41, December 2023, pp. 16-36

P- ISSN: 2220-5381
E- ISSN: 2710-1096

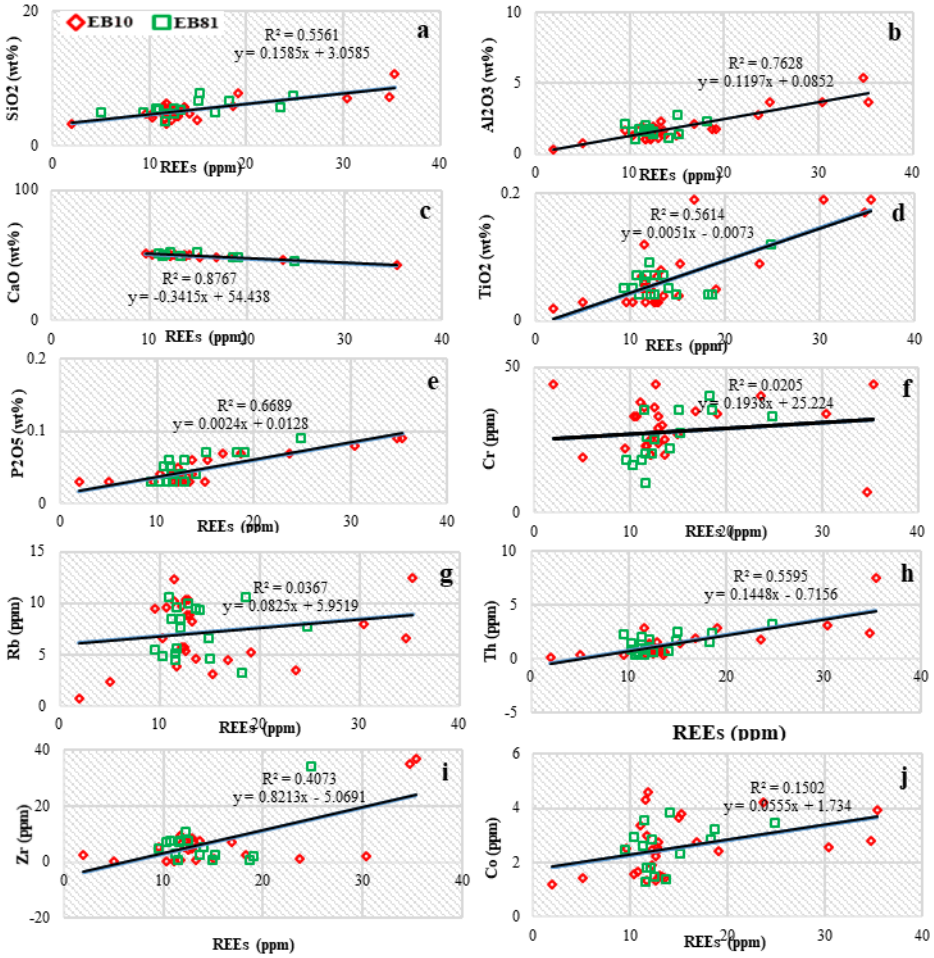

Fig. (7): Bivariate plot points for sets of (a) REEs- SiO2, (b) REEs - Al2O3, (c) REEs- CaO, (d) REEs - TiO2, (e) REEs – P2O5, (f) REEs - Cr, (g) REEs - Rb, (h) REEs –Th, (i) REEs- Zr and (j) REEs- Co in Khasib Fm. limestone.

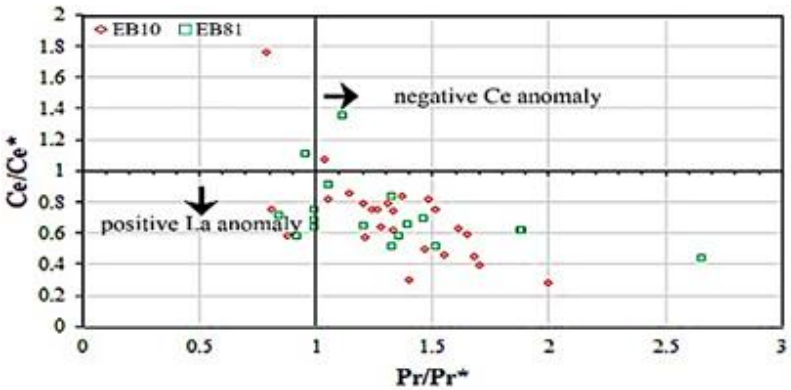

Fig. (8): Marine carbonate-normalized Pr/ Pr* vs. Ce/Ce* plot for evaluating the Ce and La anomalies using the Bau and Dulski's [16] plot for limestone of EB10 and EB81 of Khasib Formation.

Open Access
No. 41, December 2023, pp. 16-36
P- ISSN: 2220-5381
E- ISSN: 2710-1096

With respect to Al_2O_3, Th, Zr and Y, the Ce/ Ce* values exhibit positive correlations (R^2= 0.039, 0.008, 0.019 and 0.01 respectively) (Fig. 9c, d, e and f). The variety in Ce and Ce anomalies in Khasib limestone may have been influenced by terrigenous input, according to the positive correlation of Ce/Ce* ratios with Al_2O_3, Th, Zr and Y. The variability in Ce anomalies do not correspond to the paleoredox conditions of the depositional environment, according to the Ce/Ce* values' negative correlation with CaO (R^2= 0.05; Fig.9g) and U (R^2= 0.02; Fig.9h).

Thorium and uranium are primarily fractionated in an environment close to the surface, just like Ce [18]. In oxic environments, uranium is mobilized as U^{+6} and precipitates as U^{+4} in reducing environments. Both the EB10 and EB81 limestones exhibit U content (1.45-4.72 ppm and 0.85-4.42 ppm, respectively). The mobilization of U^{+6} from sediments to the surrounding water in an oxic environment is the cause of the decreasing U content in EB10 and EB81 limestones. Also used to comprehend the redox changes in the marine environment is the concentration of authigenic U (Total U- Th/3) [19]. Values of the authigenic U below 2 imply oxic deposition, while values above 2 signify dysoxic deposition. This study's limestones have authigenic U content (1.26–4.44 ppm, 0.66–4.06 ppm, respectively), which suggests that they were formed in dysoxic conditions.

4.4 Eu anomaly

Redox-sensitive elements Eu (Eu^{2+}, Eu^{3+}) and Ce (Ce^{3+}, Ce^{4+}) exhibit different geochemical behavior from those other Lantonides. In general, Eu (Eu^{2+}, Eu^{3+}) and Ce (Ce^{3+}, Ce^{4+}) are regarded as a natural proxy for redox reactions and revealing particle-solution interactions [20]. Eu anomalies "equation (2)," in the Khasib limestone have been calculated, and the results show positive anomalies ranging from 0.45 to 1.82 with a mean of 1.18; 0.66 to 1.73 with a mean of 1.22 for EB10 and EB81, respectively. Frequently favorable limestones affected by hydrothermal processes exhibit Eu anomalies (normalized to PAAS), severe diagenesis, variants in the feldspar content [11], aeolian input, too, also other variables that may lead to positive Eu anomalies in limestones. It may be governed that hydrothermal activity contributed to the occurrence of positive Eu anomalies in the Khasib limestone due to the positive correlation between Ce/Ce* and elements such as Fe_2O_3 and Mn (Fig. 9). There haven't been any indications of aeolian components in the Khasib limestone to date. Positive correlations for both Eu/ Eu* and some immobile elements, like Th, Y, and Zr, can be used to presume that diagenetic processes played a part in the occurrence of positive Eu anomalies with in limestone [20]. The pairs Eu/ Eu* -Th (R^2=0.05; Fig.10a), Eu/ Eu* -Y (R^2=0.09; Fig.10b), and Eu/ Eu* -Zr (R^2=0.15; Fig.10c) show positive correlations, which

Open Access
No. 41, December 2023, pp. 16-36
P- ISSN: 2220-5381
E- ISSN: 2710-1096

support the idea that diagenesis played a significant role in the occurrence of Eu anomalies in the Khasib limestone. Additionally, the positive correlation between both the pair of Sr-Mn can be used to infer the impact of diagenetic alteration in the limestone [2], (Fig.10d). Limestones may exhibit positive Eu anomalies as a result of detrital feldspar inclusions in sediments [13]. Different types of feldspars can be identified in sediments using oxide ratios like Na_2O/Al_2O_3 and K_2O/Al_2O_3. According to Figure 10e and 10f, the Khasib limestone exhibits negative correlations between Na_2O/Al_2O_3 and K_2O/Al_2O_3 with Eu/Eu* (R^2=0.005 and 0.02 respectively). It appears that the occurrence of positive Eu anomalies was not significantly influenced by the presence of feldspars in the studied limestone.

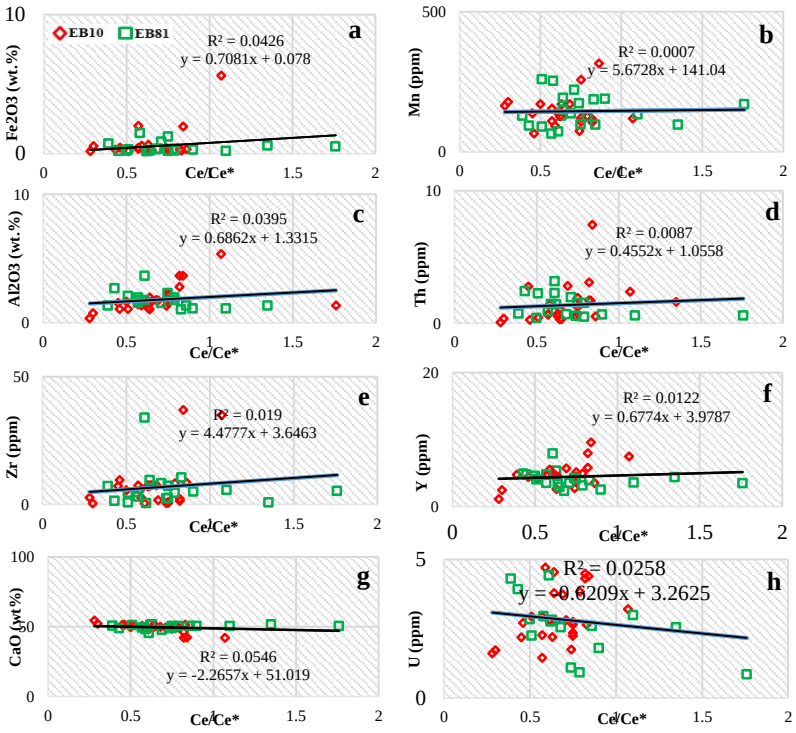

Fig. (9): Bivariate plot points for sets of (a) Ce/Ce*- Fe_2O_3, (b) Ce/Ce* - Mn, (c) Ce/Ce*- Al_2O_3, (d) Ce/Ce*- Th, (e) Ce/Ce*- Zr, (f) Ce/Ce*- Y, (g) Ce/Ce*- CaO, (h) Ce/Ce*- U in Khasib Fm. limestone.

Open Access
No. 41, December 2023, pp. 16-36

P- ISSN: 2220-5381
E- ISSN: 2710-1096

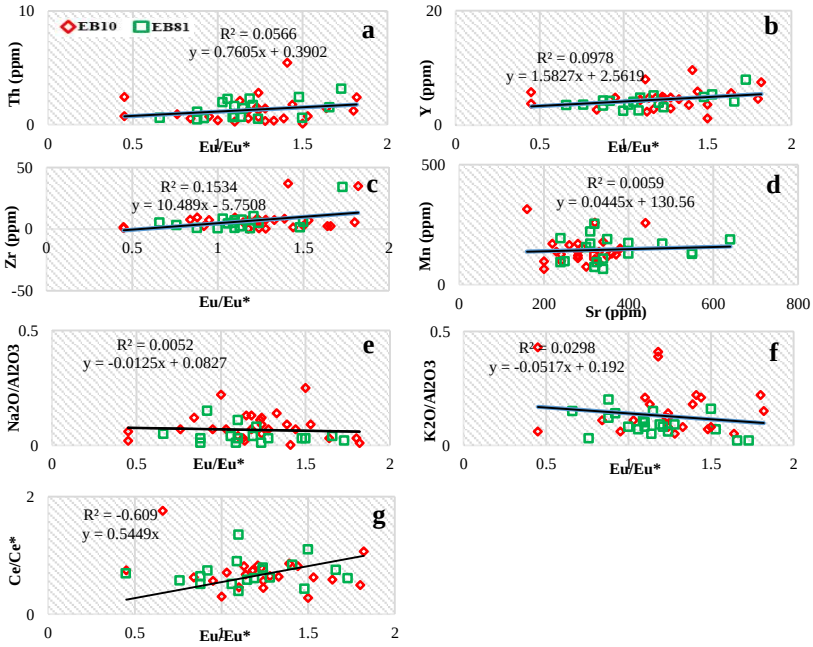

Fig. (10): Bivariate plot points for sets of (a) Eu/Eu*- Th, (b) Eu/Eu*- Y, (c) Eu/Eu*- Zr, (d) Sr- Mn, (e) Eu/Eu*- Na_2O/Al_2O_3, (f) Eu/Eu*- K_2O/Al_2O_3, (g) Eu/Eu*- Ce/Ce* in Khasib Fm. limestone.

4.5 The limestones' Y/Ho, Er/Nd and La_N/ Yb_N ratios

Research on REEs, especially LREE from marine sediments, may provide insight into the original properties of seawater. Seawater typically has elevated Y/Ho ratios 44–74, terrigenous materials always have Y/Ho ratios of 28 [1]. In open sea water, the Y/Ho ratio usually ranges between 60 and 90, but it is highly influenced by salinity. Compared to freshwater carbonates, marine carbonates exhibit higher Y/Ho ratios [2]. The limestones of the Khasib Formation in the current study exhibit wide variations in Y/Ho ratios (23.25-57.5 with an average of 35.19 for EB10 and 18.0-53.0 with an average of 31.54 for EB81), suggesting input from the surface. The Er/Nd ratio can be used to illustrate the effects of LREE/HREE fractionation in both present and historic marine systems. In typical seawater, the Er/Nd ratio is around 0.27.

The seawater certificate that the marine carbonate has preserved and successfully indicated by the rising Er/Nd ratio of limestones. Due to the favorable concentration of Nd compared to Er, addition of diagenesis or detrital material can lower the Er/Nd value to less than 0.1. The Khasib limestones' Er/Nd ratios range from 0.09 to 0.2 for EB10 and 0.12-0.17 for EB81, further demonstrating the impact of detrital material. La_N/Yb_N ratios in the limestones exhibit very minor variations (Table

Open Access
No. 41, December 2023, pp. 16-36
P- ISSN: 2220-5381
E- ISSN: 2710-1096

4). The values presented by Madhavaraju and Gonzalez-Leon [18] (about 1.0) for terrigenous materials, are remarkably near to the La_N/Yb_N ratios of Khasib limestone. As a result, the studied limestones exhibit a seawater-like REE+Y pattern with an enrichment of HREE relative to LREE and are contaminated with terrigenous materials.

5. Conclusions

1- Minor variations exist in the concentrations of major, trace, and REE in the Khasib limestones of the EB10 and EB81. Terrigenous input and scavenging process governed both positive and negative Ce anomalies as well as the observed variations in Ce and Ce anomalies in these limestones. The limestones in this study have increasing levels of U and authigenic U, which indicates that dysoxic conditions were present when they were formed. The limestones have low ∑REE components, high Y/Ho ratios, low Er/Nd ratios, La_N/Yb_N ratios close to 1, and seawater-like REE+Y patterns, which indicate that the REE concentrations were primarily derived from seawater, with the inclusion of terrigenous input. Strongly positive correlations between REEs and SiO_2, Al_2O_3, TiO_2, P_2O_5, Cr, Rb, Th, Zr, and Co, as well as a negative correlation between REEs and CaO, provide additional evidence for this claim.

2- The positive correlations among Ce/Ce* and elements such as Fe_2O_3, Mn, Al_2O_3, Th, Zr, and Y as well as the negative correlations between Ce/Ce* and some elements such as CaO and U show that detrital input significantly controlled the variation in values of Ce anomalies in the limestone. Additionally, the previously stated negative correlations provide a compelling justification for the limestone's deposition in a shallow marine environment.

3- The strong correlations between Eu/Eu* and elements like Th, Y, and Zr led us to draw the conclusion that diagenetic processes were responsible for the positive Eu anomalies in the Khasib limestone.

4- Low Er/Nd values and positive correlations between Eu/Eu* and Ce/Ce* show that diagenetic fluids played a significant role in determining the concentration of REEs in the limestone.

Open Access
No. 41, December 2023, pp. 16-36
P- ISSN: 2220-5381
E- ISSN: 2710-1096

References

[1] S. R. Taylor and S. H. McLennan, "The geochemical evolution of the continental crust", *Review Geophysics*, v. 33, pp. 241-265, 1985.

[2] A. Abedini and A. A. Calagari, "Rare earth element geochemistry of the Upper Permian limestone: The Kanigorgeh mining district, NW Iran", *Turk. J. Earth Sci*., vol. 24, no. 4, pp. 365–382, 2015. https://doi.org/10.3906/yer-1412-30

[3] M. S. Abbas, M. H. Khudhair, and O. S. Al-Saadi, "Electro-Facies and Petrophysical Properties of the Hartha Formation in Selected Wells of East Baghdad Oil Field", Iraqi Journal of Science, vol. 63, no. 3, pp. 1129–1145, Mar. 2022. https://doi.org/10.24996/ijs.2022.63.3.20

[4] A. K. Al-Temimi, "Reservoir Characterization of East Baghdad Oil field, Iraq, " *Indian J. of Natural Sciences*, 9: 51, 2018.

[5] B. A. H. Al-Baldawi, "Using Well Logs Data in Logfacies Determination by Applying the Cluster Analysis technique for Khasib Formation, Amara Oil Field, South Eastern Iraq", Journal of Petroleum Research and Studies, vol. 6, no. 2, pp. 9-26, Jun. 2016. https://doi.org/10.52716/jprs.v6i2.146

[6] M. I. Abdel-Fattah, A. Q. Mahdi and M.A. Theyab, "Lithofacies classification and sequence stratigraphic description as a guide for the prediction and distribution of carbonate reservoir quality: A case study of the Upper Cretaceous Khasib Formation (East Baghdad oilfield, central Iraq)", *J. of Petroleum Science and Engineering*, vol. 209, 109835, 2022. https://doi.org/10.1016/j.petrol.2021.109835

[7] L. A. Jameel, F. S. Kadhim, and H. I. Al-Sudani, "Geological Model for Khasib Formation of East Baghdad Field Southern Area", Journal of Petroleum Research and Studies, vol. 10, no. 3, pp. 21-35, Sep. 2020. https://doi.org/10.52716/jprs.v10i3.327

[8] T. A. Mahdi and A. A. M. Aqrawi, "Sequence Stratigraphic Analysis of the Mid-Cretaceous Mishrif Formation, Southern Mesopotamian Basin, Iraq", *J. of Petroleum Geology*, vol. 37, no. 3, pp. 287-312, July 2014. https://doi.org/10.1111/jpg.12584

[9] T. K. Al-Ameri and R. Y. Al-Obaydi, "Cretaceous petroleum system of the Khasib and Tannuma oil reservoir, East Baghdad oil field, Iraq, " *Arab J Geosci*, vol. 4, pp. 915–932, 2011. https://doi.org/10.1007/s12517-009-0115-4

Open Access
No. 41, December 2023, pp. 16-36
P- ISSN: 2220-5381
E- ISSN: 2710-1096

[10] K. K. Turekian and K. H. Wedepohl, "Distribution of elements in some major units of earth's crust: Geological Society of America Bulletin", vol. 72, no. 2, pp. 175-192, 1961. https://doi.org/10.1130/0016-7606(1961)72[175:DOTEIS]2.0.CO;2

[11] M. Ozyurt, M. Z. Kirmaci, I. Al-Aasm, C. Hollis, K. Tasli and R. Kandemir, "REE Characteristics of Lower Cretaceous Limestone Succession in Gümüşhane, NE Turkey: Implications for Ocean Paleoredox Conditions and Diagenetic Alteration", *Minerals*, vol.10, no. 8, p.683, 2020. https://doi.org/10.3390/min10080683

[12] Y. Deng, J. Ren, Q. Guo and J. Cao, "Rare earth element geochemistry characteristics of seawater and pore water from deep sea in western Pacific, "*Sci. Rep.*, vol. 7, 16539, 2017. https://doi.org/10.1038/s41598-017-16379-1

[13] J. Madhavaraju, H. Löser, Y. Lee and R. Santacruz, "Geochemistry of Lower Cretaceous limestones of the Alisitos Formation, Baja California, México: Implications for REE source and paleo-redox conditions", *J. of South American Earth Sciences*, vol. 66, pp. 149-165, 2016 https://doi.org/10.1016/j.jsames.2015.11.013

[14] K. Zhang and G.A. Shields, "Sedimentary Ce anomalies: Secular change and implications for paleoenvironmental evolution", *Earth-Science Reviews*, vol. 229, 104015, 2022. https://doi.org/10.1016/j.earscirev.2022.104015

[15] M. Bau and A. Koschinsky, "Oxidative scavenging of cerium on hydrous Fe oxide: Evidence from the distribution of rare earth elements and yttrium between Fe oxides and Mn oxides in hydrogenetic ferromanganese crusts, "*Geochemical journal*, vol. 43, no. 1, pp. 37-47, 2009. https://doi.org/10.2343/geochemj.1.0005

[16] M. Bau and P. Dulski, "Distribution of yttrium and rare-earth elements in the Penge and Kuruman iron formations, Transvaal Supergroup, South Africa", *Precambrian Research*, vol.79, no. 1-2, pp. 37-55, 1996. https://doi.org/10.1016/0301-9268(95)00087-9

[17] H. Zhang, J. Zhou, P. Yuan, Y. Dong and W. Fan, F. Chu, W. Xiao, and D. Liu, "Highly positive Ce anomalies of hydrogenetic ferromanganese micronodules from abyssal basins in the NW and NE Pacific: Implications for REY migration and enrichment in deep-sea sediments", *Ore Geology Reviews*, vol. 154, 105324, 2023. https://doi.org/10.1016/j.oregeorev.2023.105324

[18] J. Madhavaraju and C.M. González-León, "Depositional conditions and source of rare earth elements in carbonate strata of the Aptian-Albian Mural Formation, Pitaycachi

Open Access
No. 41, December 2023, pp. 16-36
P- ISSN: 2220-5381
E- ISSN: 2710-1096

section, northeastern Sonora, Mexico", *Revista Mexicana de Ciencias Geológicas*, vol. 29, no. 2, pp. 463-477, 2012.

[19] M.O. Clarkson, R. Hennekam, T.C. Sweere and M.B. Andersen, "Carbonate associated uranium isotopes as a novel local redox indicator in oxidatively disturbed reducing sediments", *Geochimica et Cosmochimica Acta*, vol. 311, pp. 12-28, 2021. https://doi.org/10.1016/j.gca.2021.07.025

[20] G.A. Shields and G.E. Webb, "Has the REE composition of seawater changed over geological time?", *Chem. Geol.*, vol. 204, pp. 103-107, 2004. https://doi.org/10.1016/j.chemgeo.2003.09.010